FINITE ELEMENT ANALYSIS OF BREAKOUT FORCE OF OBJECTS EMBEDDED IN SEA BOTTOM

Mosleh A. Al-Shamrani

College of Engineering, King Saud University,
P.O.Box 800, Riyadh 11421, Saudi Arabia

ABSTRACT

The paper presents a finite element analysis of the force required to lift objects embedded in cohesive seafloor sediments. The behavior of the soil is described by a broadly applicable time-dependent constitutive model for cohesive soils. The validity of the numerical solution is evaluated by comparing the calculated breakout force with predictions obtained from some available empirical and analytical equations. In addition, the failure mechanism developed during the breakout of an embedded object is examined, and influence of soil characteristics, shear strength in particular, on the magnitude of the breakout force is investigated. The presented analyses demonstrate that the finite element solution for the breakout force is satisfactory and in a qualitative agreement with estimates from other methods. Therefore, the finite element method can provide a useful tool for studying the breakout phenomenon, and has a potentially broad realm of application that allows one to evaluate the effect of various factors on the magnitude of the breakout force required to free an embedded object.

1. INTRODUCTION

Increased interest in exploration and utilization of marine resources has led to the construction of different civil-engineering type structures in the ocean. Frequent mobility of such offshore structures as well as the need for providing reliable anchors and mooring systems for ships and surface or submerged platforms has resulted in special attention being focused on the evaluation of the force required to lift an object embedded in sediments of the ocean floor (Muga, 1967; Vesic, 1971). In offshore engineering terminology the portion of this force in excess of the object submerged weight is commonly called the breakout force (Muga, 1967; Finn and Byrne, 1972; Lee, 1973), the net breakout force (Liu, 1969), or the breakout resistance (Rapoport and Young, 1985).

For cohesionless sediment the force required to lift an embedded object will approximately be equal to its submerged weight (Lee, 1973). This is also the case when the object rests on the seafloor without embedment and no adhesion develops between the object and the deposit in which it is embedded. In fact, Lee (1973) pointed out that, for embedment depth less than one-tenth the object width, breakout force is almost negligible. If, however, the object is embedded enough into a cohesive sediment then upon applying the upward force skin friction develops along the surface area of the object and adhesion develops beneath the object. In addition, if the breakout force is rapidly increased such that water has no time to flow into or through the underlying soil then suction force, which is considerably higher than the adhesion, develops below the object. It is this force that comprises the major portion of the breakout force. Researchers agree that the major part of the applied force is to overcome this suction force.

Depending on extent of embedment, buried objects may be categorized into partially or totally embedded. In case the embedment is greater than the width of the object then the breakout may take place through general failure of the soil above the base of the object, and the breakout force can be estimated from available techniques developed for embedded anchors (Lee, 1973; Rapoport and Young, 1985). If, on the other hand, the object is embedded by an amount less than its width, it is considered to be partially embedded and the breakout force is controlled by the force below the base of the object (i.e., suction) whose magnitude is a function of embedment, rate of loading, and soil properties.

The problem of breakout force has commonly been subdivided into two problems. In the first class the concern is on the estimation of the force required to pullout the object in a very short time. This force is termed the immediate breakout force (Lee, 1973). In another class, the objective is to find the time at which the object can be dislodged from the sediment if a breakout force less than the immediate breakout force is applied. Of course, the smaller the magnitude of the applied force the longer is the time required for breakout. Therefore, in the immediate case the time for breakout is known and the value for the immediate breakout force is required whereas for long-term case the force for breakout is predetermined and the time for breakout is required.

Limited information is available on the breakout behavior of objects embedded in seafloor. Evaluation of the breakout force still relies on empirical correlations that are obtained based on the results of limited field and laboratory pullout tests. In the few attempts that have so far been made to apply soil mechanics to the breakout problem the soil behavior is considered to be elasto-plastic (Muga, 1968) or perfectly plastic (Finn and Byrne, 1972; Byrne and Finn, 1978; Rapoport and Young, 1985). There is, however, an overwhelming experimental evidence that saturated clay soils do behave like viscoplastic materials. This is especially the case for many ocean-bottom sediments where their properties, including strength, are strongly time-dependent because of the semiliquid and liquid consistency of those deposits (Muga, 1967). It is, therefore, doubtful that a truly realistic estimate of the breakout force can be obtained from inviscid analysis.

In this paper, the use of a broadly applicable time-dependent constitutive model, implemented in a finite element code, in estimating the force required for extracting partially embedded objects in cohesive seafloor soils is demonstrated. The model formulation is general and it describes the elastoplastic-viscoplastic, path-dependent, rheological, and nonlinear stress-strain-strength properties of cohesive soils under general loading conditions. Consideration is restricted here to the immediate breakout problem. The general validity of the numerical solution for the case when a breakout force less than the immediate breakout force is applied has been considered elsewhere (Al-Shamrani, 1995).

Focus is limited to the behavior of fully saturated clay-object interaction where the pullout is assumed to occur with no volume change (i.e., undrained analysis). Results of the numerical solution are compared with those obtained from some currently available analytical and empirical correlations. In addition, the mode of failure developed during the breakout of an embedded object is examined, and influence of soil characteristics, namely; its undrained shear strength, on the magnitude of the breakout force is evaluated.

2. PREVIOUS STUDIES

The breakout phenomenon has been the subject of a number of experimental and analytical investigations. The first, and by far the most comprehensive, is the laboratory and field experimental studies carried out in the late 1960s by the US Naval Civil Engineering Laboratory (*NCEL*) in Port Hueneme, California. In this testing program, tests were conducted on various shaped objects with a submerged weight up to about 90 KN. Muga (1967) reported the results of the first phase of this investigation and proposed the following empirical equation for the upward force applied to objects embedded in San Francisco Bay mud to cause immediate breakout

$$F_{lib} = 0.81AF_q + W'' \tag{1}$$

Where F_{lib} is the applied force, or what Lee (1973) has called the immediate breakout line force. The W'' is the object weight when submerged in the sediment. It is equal to its buoyant weight minus the buoyant weight of the soil displaced by the object. A is the object plan area in contact with soil and F_q is taken as a measure of the downward bearing capacity of the soil, however, Muga neither specified its magnitude nor how it would be evaluated. It should be stated that most of the symbols used by Lee (1973) are adopted in this paper since we found them to be a very consistent and comprehensive set of notation.

Liu (1969) presented the results reported by Muga along with the results of laboratory model tests and field tests conducted in the Gulf of Mexico. He proposed a correlation that takes into account breakout time as well as the time the object has been embedded in the sediment. Lee (1973) reanalyzed the same data and from the best-fit of the experimental results he suggested a correlation between F_{lib} and the compressive bearing capacity such that

$$F_{lib} = 1.5A\left[\left(1 - 0.97e^{-2.75D_f/B}\right)F_q\right] + W'' \tag{2}$$

Where B is the object width and D_f represents the depth of embedment. Lee proposed that F_q is the compressive load carried by the sediment immediately before breakout and is obtained from the conventional Skempton (1951) bearing capacity equation, or

$$F_q = 5S_u\left(1 + 0.2\,\frac{D_f}{B}\right)\left(1 + 0.2\,\frac{B}{L}\right) \tag{3}$$

Where S_u is the undrained shear strength of soil and L is the length of object. In case the ratio D_f/B is greater than 0.25 and the object sank slowly, Lee suggested that F_q may be taken as the buoyant weight of the object minus the submerged weight of the soil displaced by the object (i.e., $F_q = W''$).

Based on earth pressure theory and the expansion of cavities, Vesic (1971) presented an analytical analysis of the breakout pressure for a fully embedded plate anchor found at depth D below the surface. Suction forces developed at the object-soil interface are assumed to be zero and time effects are included indirectly through soil properties.

Finn and Byrne (1972) postulated that, if during pullout a high suction developed underneath the base of the embedded object, the failure mechanism of breakout problem is similar to the mechanism of shallow footing loaded in compression. Based on this hypothesis, the following modified bearing capacity equation was proposed

$$F_{lib} = \left(S_u N_c - \gamma' D_f\right) A + W_b \qquad (4)$$

where N_c is a bearing capacity factor which depends on the shape of the object, γ' is sediment submerged unit weight, and W_b is the submerged weight of the object in water. Using this equation to predict the results of *NCEL* tests, Finn and Byrne found N_c to be in the range of 2.8 to 9.4 for a cube object and 5.4 to 17.9 when the object is a rectangle. It is to be noted that the calculated N_c is substantially higher than the theoretical value which according to the plasticity theory should be between 5.2 and 6.2 depending on the shape of the object. It appears, however, that Finn and Byrne used an incorrect area for the rectangular object, and when using the correct area N_c ranges between 2.2 and 5.9 (Craig and Chua, 1990).

Byrne and Finn (1978) further examined the validity of their hypothesis by conducting rapid laboratory tests on 25-mm-diameter footings embedded in silty clay. It was found that breakout took place due to failure of the supporting soil and was not due to breakdown in adhesion between the soil and the object. However, it should be mentioned that there was 6-mm-deep skirts along the perimeter of the object which is believed to have an effect on the observed failure mechanism. Instead of using Eq. 4 in predicting the test results, Byrne and Finn used the Hansen bearing capacity equation (Bowles, 1982), and N_c was found to range between 6.5 and 7.4.

Roderick and Lubbad (1975) conducted a set of laboratory tests where effect of object in-situ time on the value of breakout force was investigated. It was observed that a conical soil mass adhered to the base of the object and moved with it for almost all tests. Based on the results of laboratory model tests, Rapoport and Young (1985) confirmed the similarity between downward and upward undrained loading of cohesive soils. However, similar to Finn and Byrne (1978) tests, suction breakdown was prevented with a skirt along the perimeter of the object. It was also found that when sufficient time is available for free drainage to relieve underbase suction failure takes place close to the soil-object interface.

Using centrifuge model tests, Craig and Chua (1990) investigated uplift forces for offshore foundations embedded in clay soils. Results indicated that if the downward bearing stresses exceed about four times the undrained shear strength, then substantial suction forces developed underneath the object. This in turn leads to high breakout forces that could reach the compressive bearing capacity of the soil.

It is obvious that the breakout problem has been the subject of a number of field and laboratory investigations. Certainly, each approach has its own merits and limitations. The main disadvantage of laboratory model tests is the extrapolation of the data to large objects and the difficulty involved in preparing soil layer that represents the actual field sediment. Field testing, on the other hand, is more reliable as it directly reflects the effect of shape and size of the object. However, interpretation of results is complicated by the nonhomogeneity of the sediment, and hence the wide varieties in its engineering properties. Furthermore, due to high

expense involved in conducting full scale breakout tests, available field data are limited and further data are unlikely to be obtained soon.

Therefore, utilizing another procedure for the analysis of the breakout problem is considered desirable. The complexity of the problem dictates the method of analysis be numerical in nature. Although Muga (1968) has presented a numerical procedure for solving the breakout problem, the solution is based on elasto-plastic soil properties and this represents extreme simplification of marine sediments pronounced time-dependent behavior. There does not seem to have been any analytical or numerical solution in which the breakout problem is analyzed with the nonlinear and rheological behavior of soil taken into consideration. The constitutive model used in this study takes into account the elasto-plastic, rheological, and anisotropic behavior of marine soil. Therefore, it is well qualified to be used in the analysis of various offshore soil-structure problems, among of which is the breakout problem considered in this paper.

3. FINITE ELEMENT ANALYSIS OF THE BREAKOUT PROBLEM

For the purpose of illustration, analysis is limited to the behavior of a fully saturated clay-object interaction and the pullout is assumed to occur with no volume change. Consequently, the evaluated pullout force is the immediate breakout force, and it represents the upper limit for the breakout force. In reality, this case takes place when the breakout force is applied so rapidly and the soil permeability is too low to allow for significant water flow into or through the underlying soil. It is further assumed that the suction between the object base and the surrounding soil medium is large enough to ensure no separation of the object and the surrounding soil. Moreover, no cracking is assumed to occur in the material when subjected to tensile stresses.

The analysis is performed for a rectangular block embedded in a saturated cohesive sediment. The object-soil system is defined schematically in Fig. 1. The object unit weight is taken to be equal to 30 kN/m^3 and it has the following geometric characteristics: width, B = 2 m, depth, D = 2 m, length, L = 8 m. The problem geometry is transposed into two-dimensions by assuming that deformation occurred in plane strain. The two-dimensional finite element representation of the object and surrounding soil is shown in Fig. 2. The depth of submergence h is immaterial and need not be specified. Due to symmetry, only one-half of the object-soil system is discretized. The grid consists of 99 nodes and 80 isoparameteric quadrilateral elements.

The stress-strain behavior of the embedded object is assumed to be linear elastic with the properties E = 1.0 x 10^8 kN/m^2 and ν = 0.0, where E is the Young's modulus and ν is the Poisson's ratio. The value of E is selected large enough such that the object deformation is negligible, and hence the object vertical displacement represents the net upward movement. The behavior of the sediment is described by the time-dependent bounding surface model for anisotropic cohesive soils (Al-Shamrani and Sture, 1994; 1997). The model formulation is general and it describes the elastoplastic-viscoplastic, path-dependent, time-dependent and nonlinear stress-strain-strength properties of anisotropic cohesive soils under general loading conditions. Details of the formulation of the model can be found in Anandarajah and Dafalias (1986) and Al-Shamrani and Sture (1997). The model is implemented into

the finite element computer program *SAC-2* developed by Herrmann and Mish (1983). This program has the capability for analyzing quasi-static problems under plane strain, plane stress, or axisymmetric conditions.

Rather than assigning any values for the model parameters, it was found more appropriate to use values that represent the behavior of San Francisco Bay mud since the empirical correlations expressed in Eqs. 1 and 2 have been based on the results conducted for objects embedded in this sediment. However, triaxial test data required by the constitutive model are not available for the soils at the site of *NCEL* breakout tests. Therefore, we take the required parameters from the set of laboratory data reported by Bonaparte and Mitchell (1979) for San Francisco Bay mud at Hamilton Air Force Base.

Estimated Immediate Breakout Force

The load-displacement response obtained by the finite element analysis is shown in Fig. 3. With no distinct failure observed, a displacement of about 10% of the width of the object was adopted as the critical displacement. *A* value in this range has usually been selected for numerical evaluation of the compressive bearing capacity of shallow foundations. Shown also in Fig. 3 are the predicted immediate breakout line forces, F_{lib}, obtained from Eqs. 1, 2, and 4.

It is noted that the numerically found immediate breakout line force is higher than the values obtained from the empirical and analytical formulas. It is clear, however, that the difference between the finite element prediction and estimates of Eqs. 1, 2, and 4 will depend, in part, on the value adopted as a critical displacement for the numerical solution. Furthermore, the finite element estimate is considered fairly good knowing the fact that Eq. 2, for instance, predicts immediate breakout forces that could be plus or minus fifty percent higher or lower than the measured values (Lee, 1973).

Estimates of Eqs. 1, 2, and 4 are found to be largely dependent on the form of the equation used for evaluating the downward bearing capacity of the sediment. For instance, Fig. 4 is similar to Fig. 3 except that in obtaining Fig. 4 instead of making use of Eq. 3, F_q and N_c are calculated from the Hansen bearing capacity equation (Bowles, 1982). It is obvious that the numerical solution compared well with the prediction of Eq. 2. If, on the other hand, F_q is evaluated from the Terzaghi bearing capacity equation (Bowles, 1982), the finite element solution approaches the estimate obtained from Eq. 1 as shown in Fig. 5.

Predictions of Eq. 4 are, however, consistently lower than both the numerical and empirical estimates. This is irrespective of the used form for the bearing capacity equation (i.e., the value of N_c). It follows from Figs. 3, 4, and 5 that a value for N_c higher than the value used in the conventional bearing capacity equations is required in order for Eq. 4 to give a close prediction. Actually, for the object and embedment considered in this study the value of N_c for the Hansen bearing capacity equation is 7.45. Although this is slightly higher than the value of 7.4 found by Byrne and Finn (1978), still Eq. 4 significantly underestimates the breakout force. It is possible, however, that the presence of the skirts along the perimeter of the object used in Byrne and Finn tests has reduced the breakout force, and hence the calculated N_c.

Failure Mechanism for Breakout

The deformed shape at the final load increment is illustrated in Fig. 6. As might be seen, the mode of failure under pullout force is different from the known deformation pattern developed under compressive load. Here, as the object is pulled upward the soil mass outside the object moved downward and laterally towards the object while the soil beneath the object moved up. This failure pattern is in line with the mode of failure observed by Byrne and Finn (1978) except in the latter the failure zone did not extend farther away from the object. However, as we have stated above, in Byrne and Finn model tests the failure zone may have been influenced by the presence of the skirts along the perimeter of the object.

It follows from Fig. 6 that, assuming full compatibility between the object and the surrounding soil does not necessarily ensure a failure mechanism in which the soil mass beneath as well at the sides of the object will move up upon application of the pullout force. For a failure mechanism of this nature to take place a stiff soil may needed besides deep embedment and high underbase suction. It is true, however, that for a stiff deposit the embedment is more likely to be shallow. Therefore, it may safely be assumed that, a failure mode identical in pattern and direction to that for a downward loading is less likely for breakout problem. It is reasonable, however, as has been suggested by Byrne and Finn (1978) and based on the result of Fig. 6, to assume that the conventional bearing capacity and breakout problems have similar failure mechanisms but with opposite direction of motion.

Breakout Force and Soil Strength

It is obvious from Eqs. 1 through 4 that the key soil parameter involved in the breakout problem is its undrained shear strength. Fig. 7 shows the relationship between the soil undrained shear strength, S_u , and the immediate breakout line force, F_{lib}. Based on critical soil mechanics concepts the undrained shear strength of fully saturated soil is a function of its water content, or any other related property such as the void ratio. Thus, choosing different values for initial void ratio gives a corresponding set of values for S_u.

Considering this approach the results shown in Fig. 7 were obtained as follows; first a value for the initial void ratio is selected from which the unit weight, and hence the initial effective vertical and horizontal stresses are evaluated. Then, using the constitutive model a numerical triaxial test is conducted and the value of S_u is obtained. With the same set of model parameters a finite element analysis is conducted from which F_{lib} is evaluated. Finally, the value for S_u obtained from the constitutive model is used where appropriate in Eqs. 1 through 4 and the required pullout force is calculated.

From Fig. 7 it is noted, as would be expected, that F_{lib} increases with the increase in S_u . Almost the same rate of increase is seen for all methods. The finite element solution is seen to overestimate F_{lib} for all values of S_u. However, if the Hansen bearing capacity equation is used for evaluating F_q and N_c, the numerical solution approaches the predictions from Eqs. 1 and 2., for low values for shear strength as can be seen in Fig. 8. However, the numerical solution begins to deviate from the empirical estimates as S_u increases. Fig. 9 depicts the relationship between F_{lib} and S_u where in this case F_q is evaluated from the Terzaghi bearing capacity equation. It can be seen that the finite element estimate for F_{lib} is close to the

prediction of Eq. 1 at lower values for S_u but approaches the prediction of Eq. 2 as the shear strength increases.

Figs. 10, 11, and 12 compare the finite element solution and estimates obtained, respectively, from Eqs. 1, 2 and 4. It is obvious from Figs. 10 and 11 that the discrepancy between the numerical solution and the predictions of Eqs. 1 and 2 for the required applied forces depends both on the value of S_u and the bearing capacity equation from which F_q is calculated. Results of Fig. 12 indicate how Eq. 4 significantly underestimates the breakout force, irrespective of the used form of the bearing capacity equation. In order to obtain a closer estimate for the immediate breakout force, Eq. 4. should employ a value for N_c that is larger than values used for obtaining ultimate compressive bearing capacity of shallow foundations.

As has been stated at the outset of this paper, the force carried by the soil, or what is commonly called the breakout force, is the force required to extract an embedded object in excess of its submerged weight. Therefore, the immediate breakout force, F_{ib}, is simply found by subtracting the submerged weight of the object (i.e., W' for Eqs. 1 and 2 and W_b in case of Eq. 4) from the pullout line force, F_{lib}, applied to the object to cause immediate breakout.

Figs. 13, 14, and 15 show the relationship between sediment strength and immediate breakout forces obtained, respectively, from Eqs. 1, 2 and 4. Prediction from the finite element solution is included for comparison. The predictions of Eq. 4 are far below the finite element solution as shown in Fig. 15. The pattern observed in Figs. 13 and 14 is similar to that shown in Figs. 10 and 11. However, it is important to note that when F_{lb} is considered, Lee's correlation expressed in Eq. 2 always gives lower estimates than those obtained from the finite element analysis regardless of the form of bearing capacity equation used to evaluate F_q. This is in contrast to the results of Fig. 11 where it is seen that the numerical estimate could be lower than the empirical prediction of Eq. 2. The reason for this is the fact that when calculating F_{lib}, Lee (1973) has suggested a factor of safety equal to 1.5, as expressed in Eq. 2, to be applied for F_{ib}, to account for the scatter of experimental data. The results of Figs. 11 and 14 seem to support the proposition made by Lee of applying a factor of about 1.5 for immediate breakout force when calculating the required breakout force as expressed in Eq. 2.

4. SUMMARY AND CONCLUSIONS

Despite the fact that the pullout capacity of anchors found in ordinary terrestrial soil has received quite extensive investigations, limited information, however, is now available on the breakout behavior of objects embedded in seafloor soils. Evaluation of the force required to free embedded objects from ocean bottom still relies upon empirical correlations obtained from results of limited laboratory and field tests. These empirical equations have the advantage of simplicity as they include only a few selected parameters that influence the magnitude of breakout force. Their application, however, remains confined to a particular soil type, object geometry and weight, and pullout conditions.

In the present paper the breakout problem was analyzed by the finite element method. The analysis took into account both the nonlinear and rheological behavior of the surrounding soil. The validity of the numerical solution for the immediate breakout force was examined by comparison with the predictions obtained from

some available empirical and analytical equations. The present work has also provided an in-depth evaluation of the available correlations including assessment of the influence of certain factors on their predictions for the breakout force.

The presented analyses demonstrated that the finite element solution is satisfactory and in a good qualitative agreement with the predictions obtained from empirical equations. In the empirical and analytical correlations the breakout force is expressed as a function of the compressive bearing capacity of the soil. As a result, the discrepancy between the numerically calculated breakout force and those estimated from both the empirical and analytical equations considered herein was found to be dependent on the value of soil downward bearing capacity used by these equations.

The magnitude of immediate breakout force showed significant increases with increase in the undrained shear strength of the soil. Therefore, a careful determination and selection of soil strength are considered of utmost importance for a reasonable estimate of the breakout force required to free objects embedded in such a soil.

The mode of failure under pullout force was found to be different from the general failure mechanism commonly observed for compressive load, even for the case of full embedment and with the assumption of no separation between the object and soil. In other words, high suction developed at the soil-object interface does not necessarily ensure a failure mechanism in which the soil mass beneath as well at the sides of the object will move up upon application of the pullout force. It may be assumed, however, that the conventional bearing capacity and breakout problems have similar failure mechanisms but with opposite direction of motion. The most important point to be stressed here is the fact that the applicable values for the bearing capacity factor, N_c, for the two classes of problems are different and appear to be higher for the case of the breakout problem.

The presented finite element procedure appears to be capable of providing a useful tool for studying the breakout problem. It allows one to perform parametric studies and to analyze the influence of various factors on breakout force such as soil strength and deformation characteristics, object geometry and weight, extent of embedment, and pullout conditions. Further development of the numerical analysis should result in an improved method of predicting the failure mechanism that takes into account the suction force developed beneath the embedded object. Moreover, the quantitative verification of the numerical solution requires simulation of the results of well-controlled pullout model tests conducted on well-characterized material. The centrifuge modeling technique provides an excellent tool for confirmation, especially in terms of verifying the mode of failure mechanism.

REFERENCES

[1] Al-Shamrani, M. A. (1995).”Numerical Evaluation of the Breakout Force of Embedded Objects in Cohesive Seafloor Soils.” *Proc. 10th Engineering Mechanics Conference*, ASCE, Boulder, Colorado, pp. 1308-1314.

[2] Al-Shamrani, M. A. and Sture, S. (1994).”Characterization of Time-Dependent Behavior of Anisotropic Cohesive Soils.” *Proc. 8th Int. Conf. of the Assoc. for*

Computer Methods. and Advances in Geomechanics, Morgantown, WV, pp. 505-511.

[3] Al-Shamrani, M. A. and Sture, S. (1997) "A Time-Dependent Bounding Surface Model for Anisotropic Cohesive Soils." Accepted for Publication in *Soils and Foundations*, Japanese Geotechnical Society (in press).

[4] Anandarajah, A. and Dafalias, Y. F. (1986). "Bounding Surface Plasticity. III: Application to Anisotropic Cohesive Soils." *Journal of Engrg. Mech.*, ASCE, Vol. 112, No. EM12, pp. 1292-1318.

[5] Bonaparte, R. and Mitchell, J. K. (1979). "The Properties of San Francisco Bay mud at Hamilton Air Force Base, California." Geotechnical Engineering Report, University of California at Berkeley.

[6] Bowles, J. E. (1982). Foundation Analysis and Design. McGraw-Hill Book Co., New York, NY.

[7] Byrne, P. M. and Finn, W. D. L. (1978). "Breakout of Submerged Structures Buried to a Shallow Depth." *Canadian Geotechnical J.*, Vol.15, No. 2, pp. 146-154.

[8] Craig, W. H. and Chua, K. (1990)."Extraction Forces for Offshore Foundations Under Undrained Loading." *J. of Geot. Engrg.,* ASCE, Vol. 116, No. 5, pp. 868-884.

[9] Finn, W. D. L. and Byrne, P. M. (1972). "The Evaluation of the Breakout Force for a Submerged Ocean Platform." Paper OTC 1604, *Proc. 4th Offshore Tech. Conf.*

[10] Herrmann, L. R. and Mish, K.D. (1983). "Finite Element Analysis for Cohesive Soil, Stress and Consolidation Problems Using Bounding Surface Plasticity Theory." Dept. of Civ. Engrg., University of California at Davis.

[11] Lee, H. J. (1973). "Breakout of Partially Embedded Objects from Cohesive Seafloor Soils." Paper OTC 1904, *Proc. 5th Offshore Tech. Conf.*, pp. 789-795.

[12] Liu, C. L. (1969). "Ocean Sediment Holding Strength Against Breakout of Partially Embedded Objects." *Proc. Civil Engrg. in the Oceans II*, ASCE, pp. 105-116.

[13] Muga, B. J. (1967)."Bottom Breakout Forces." *Proc. Civil Engrg. in the Oceans*, ASCE, pp. 569-600.

[14] Muga, B. J. (1968)."Ocean Bottom Breakout Forces, Including Field Test Data and the Development of Analytical Method,". *Technical Report R-591*, the U.S. Naval Civil Engineering Laboratory, Port Hueneme, California.

[15] Rapoport, V. and Young, A. G. (1985). "Uplift Capacity of Shallow Offshore Foundations." *Uplift Behavior of Anchor Foundations in Soil*, ASCE, New York, N.Y., pp. 73-85.

[16] Roderick, G. L. and Lubbad, A. (1975). "Effect of Object In-situ Time on Bottom Breakout." *Paper OTC 2184, Proc. 7th Offshore Tech. Conf.,* pp. 355-359.

[17] Skempton, A. W. (1951). "The Bearing Capacity of Clays." *Proc. Building Research Congress*, London, England, pp. 180-189.

[18] Vesic, A. S. (1971).” Breakout Resistance of Objects Embedded in Ocean Bottom*.” J. Soil Mech. and Found. Engrg.*, ASCE, Vol. 97, SM9, pp. 1183-1205.

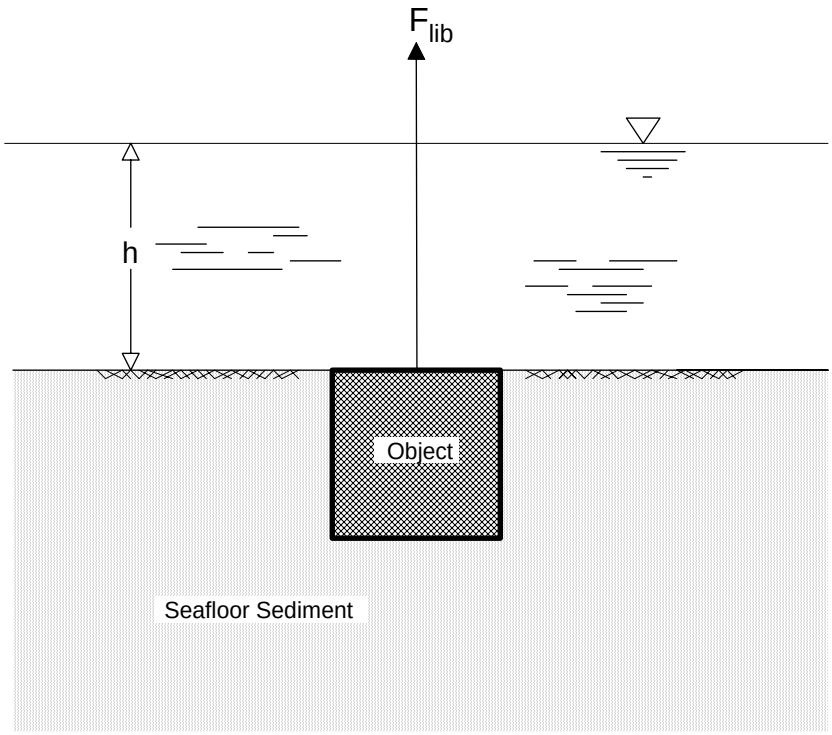

Fig. 1. Embedded Object Problem.

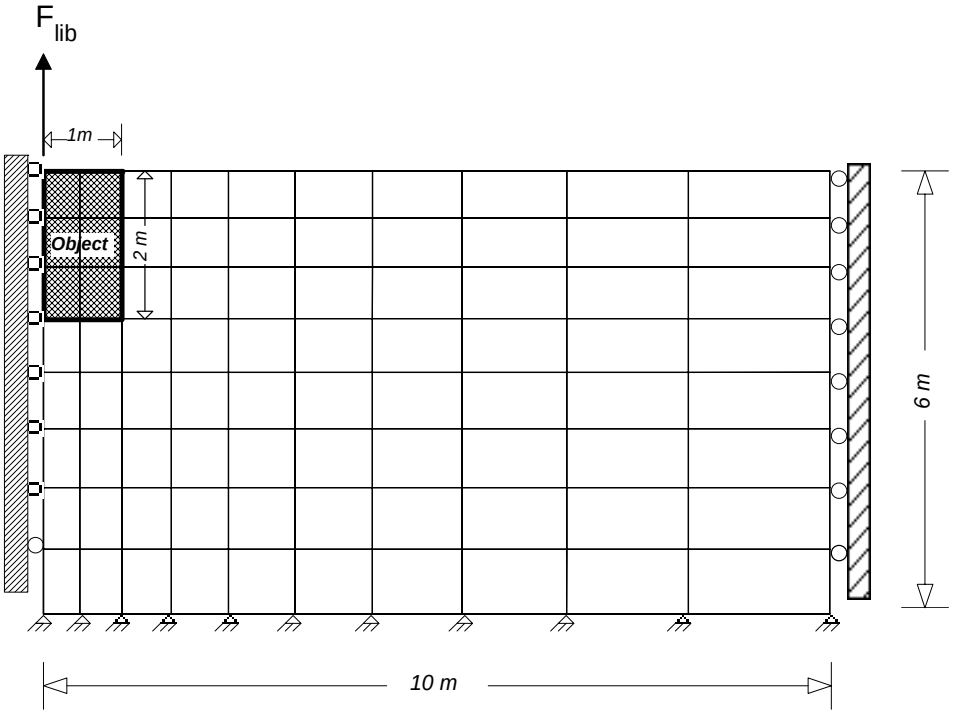

Fig. 2. Mesh Layout for the Embedded Object Problem.

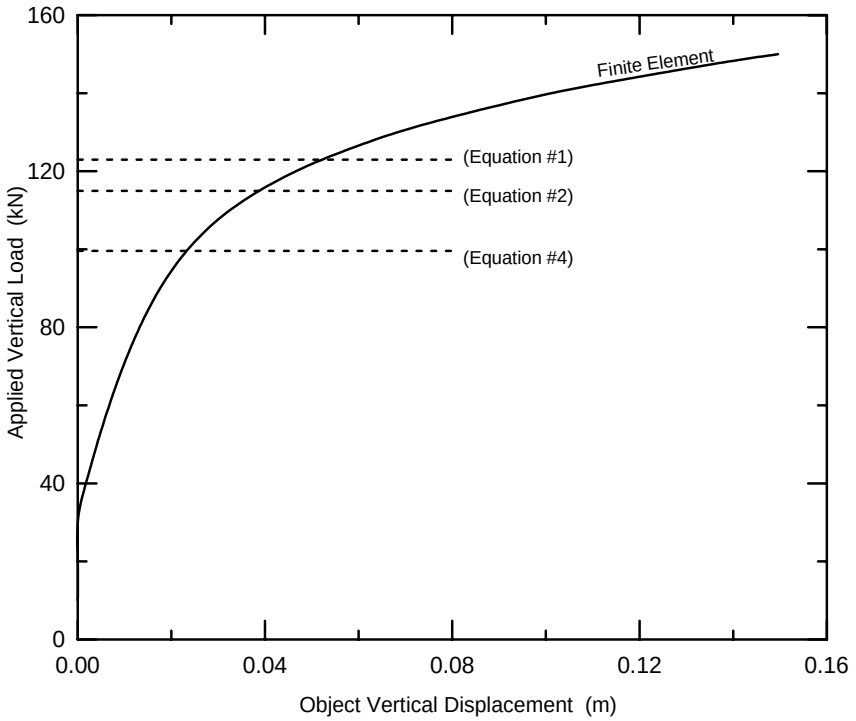

Fig. 3. Immediate Breakout line forces from finite element analysis, empirical, and analytical equations (F_q and N_c from Skempton bearing-capacity equation)

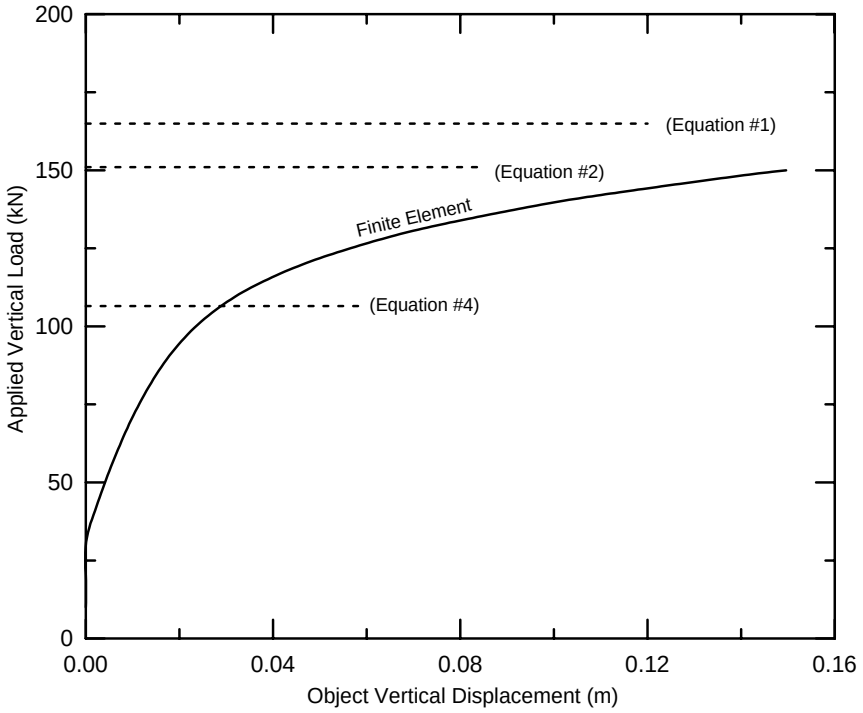

Fig. 4. Immediate breakout line forces from finite element analysis, empirical and analytical equations (F_q and N_c from Hansen bearing-capacity equation)

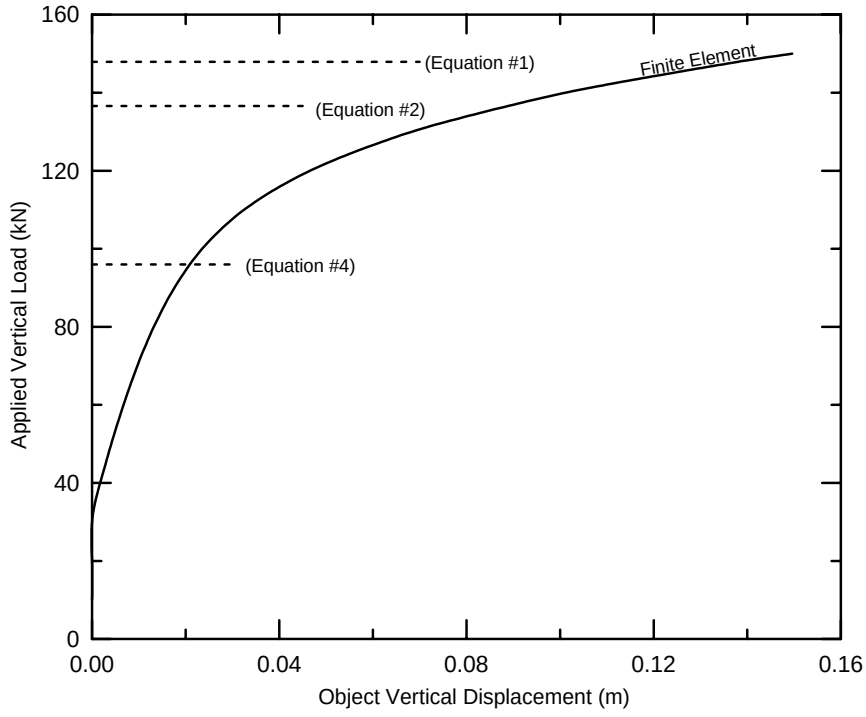

Fig. 5. Immediate breakout line forces form finite element analysis, empirical and analytical equations (F_q and N_c from Terzaghi bearing-capacity equation)

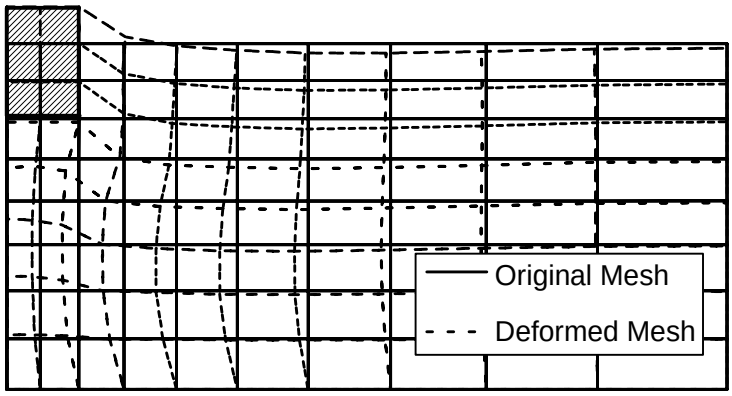

Fig. 6. Undeformed and deformed finite element meshes
(Displacements are drawn at an exagerated scale)

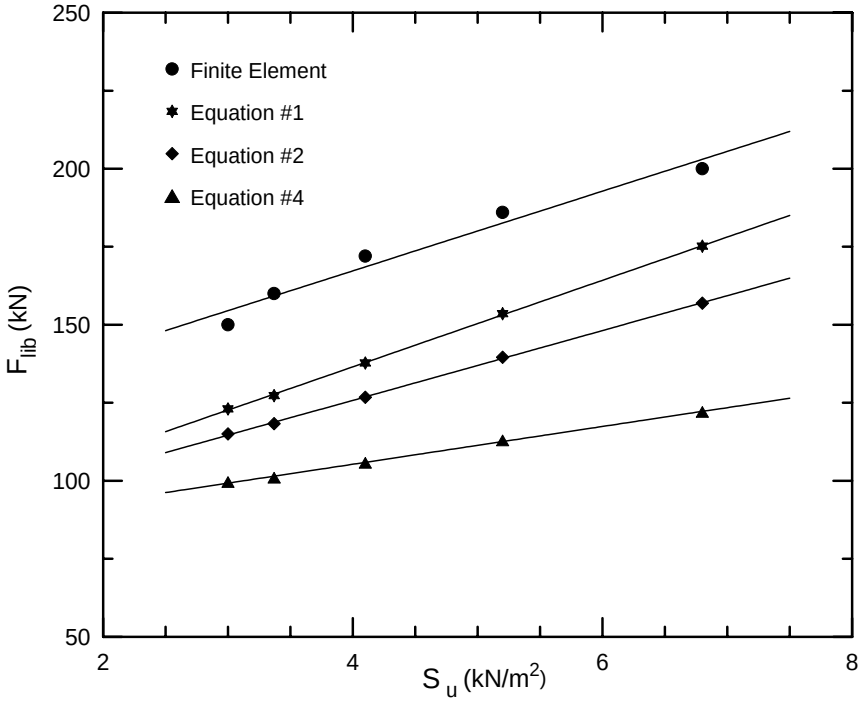

Fig. 7. Relationship between required breakout force and soil undrained shear strength (F_q and N_c from Skempton bearing-capacity equation)

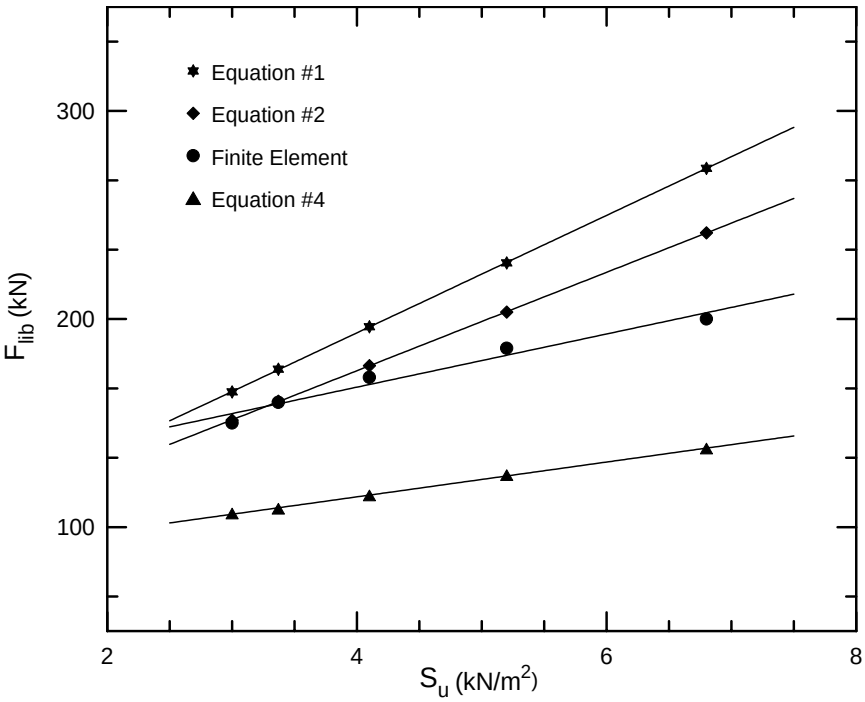

Fig. 8. Relationship between required breakout force and soil undrained shear strength (F_q and N_c from Hansen bearing-capacity equation)

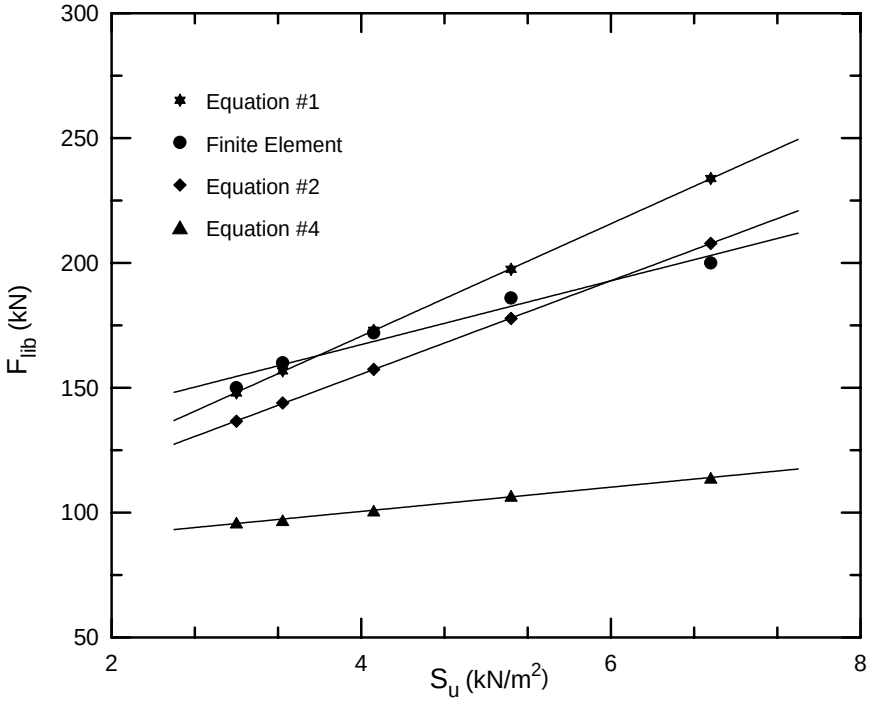

Fig. 9. Relationship between required breakout force and soil undrained shear strength (F_q and N_c from Terzaghi bearing-capacity equation)

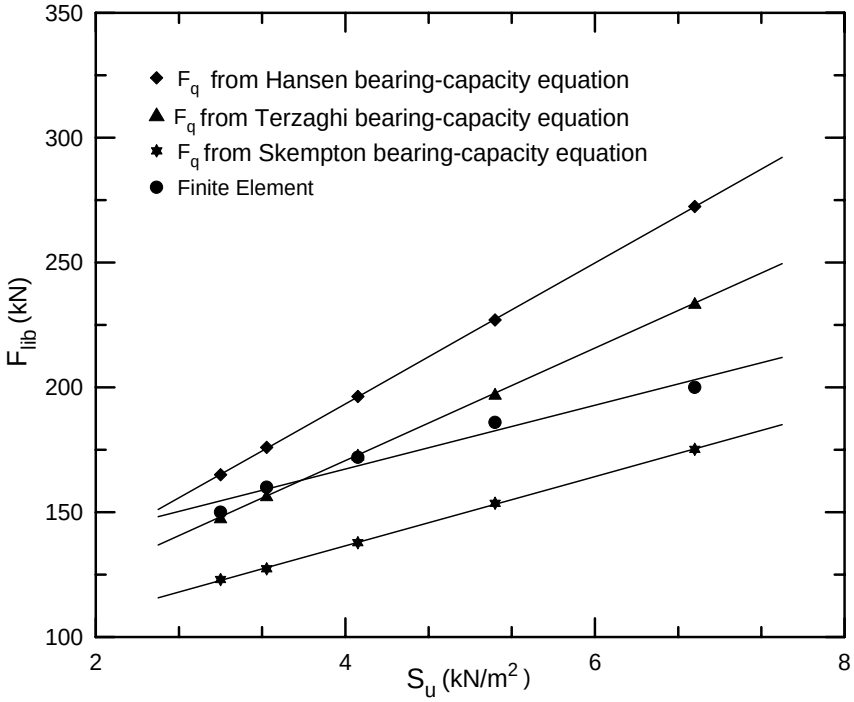

Fig. 10. Comparison: finite element and Eq. 1 solutions for immediate breakout line force.

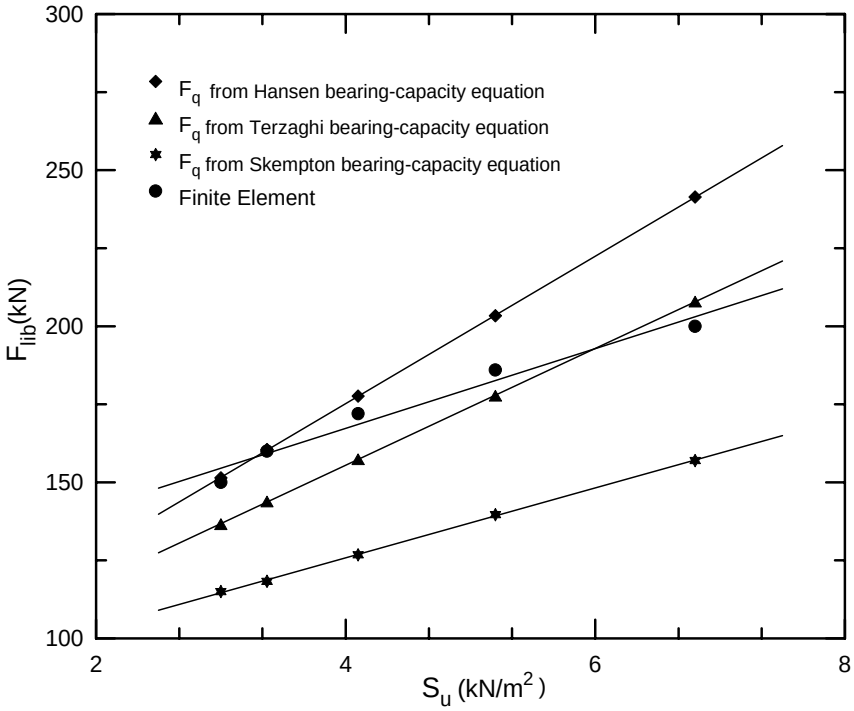

Fig. 11. Comparison: finite element and Eq. 2 solutions for immediate breakout line force.

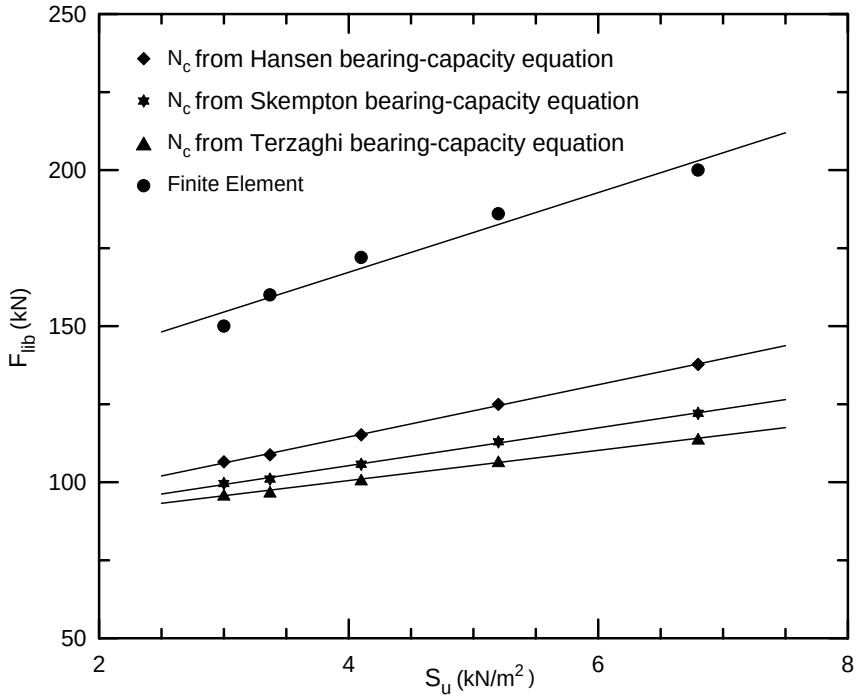

Fig. 12. Comparison: finite element and Eq. 4 solutions for immediate breakout line force.

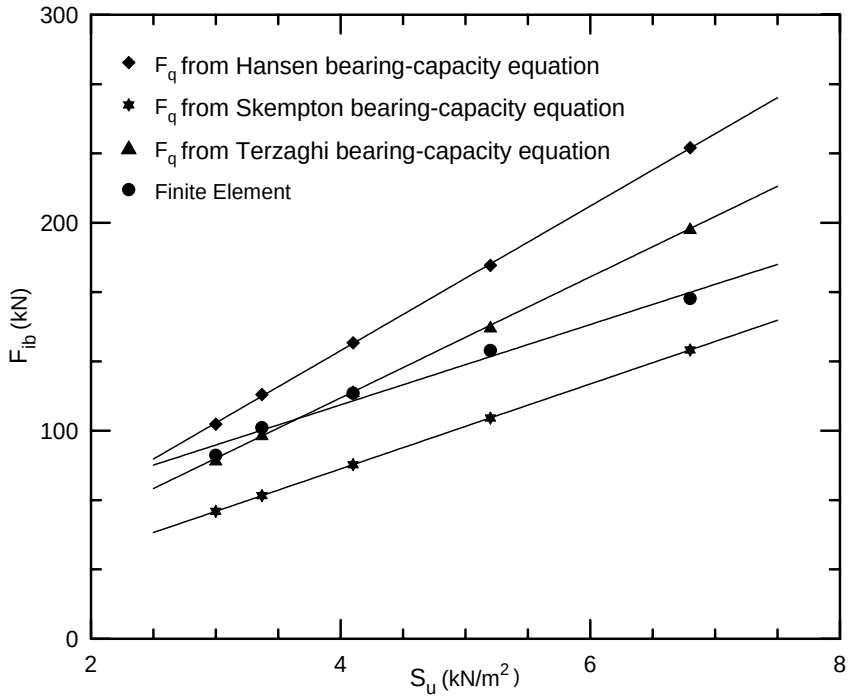

Fig. 13. Comparison: finite element and Eq. 1 solutions for immediate breakout force.

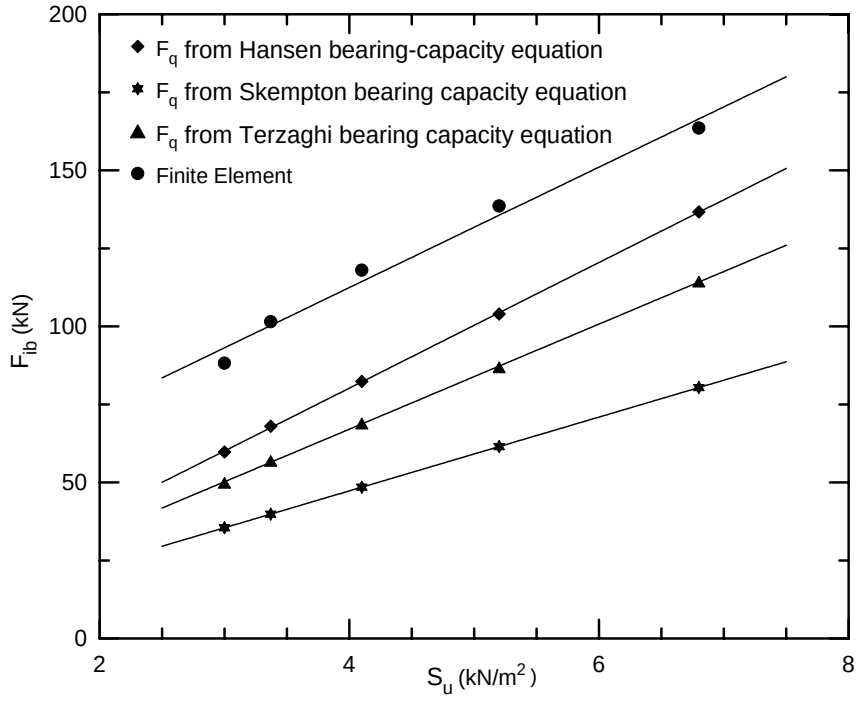

Fig. 14. Comparison: finite element and Eq. 2 solutions for immediate breakout force.

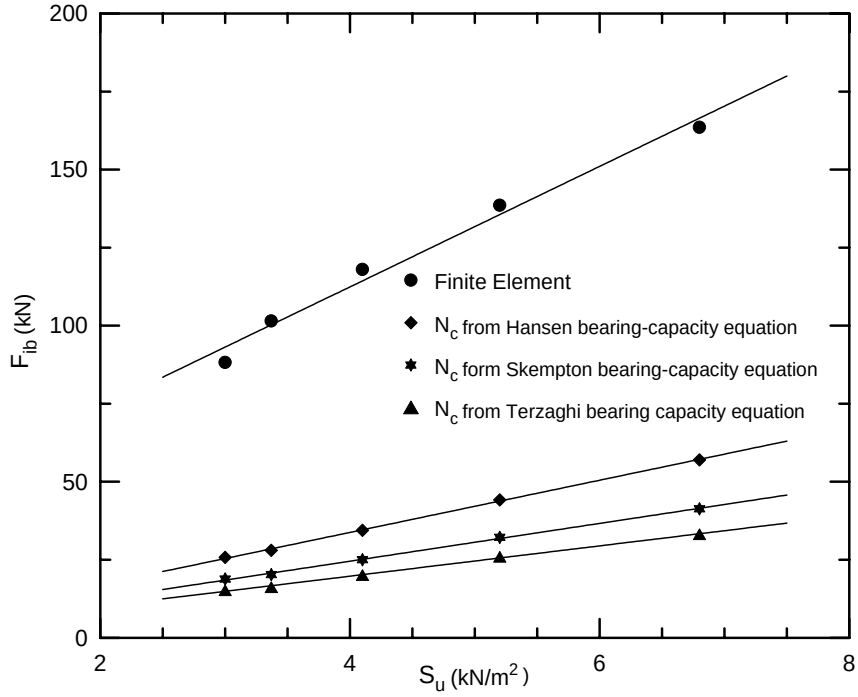

Fig. 15. Comparison: finite element and Eq. 4 solutions for immediate breakout force.